ISSN: 2414-1895 DOI: 10.6919/ICJE.202511_11(11).0017

Optimization Design of Integrated High-Temperature Valve Bonnet Heat Dissipation Structure and Orthogonal Sensitivity Analysis of Key Parameters

Dan Yao[1,*], Junxiao Sun[2], Zhenyu Lei[2], Feng Hu[1], Ruihong Ma[1], Shuangjiang Li[3]

[1] China Shipbuilding (Chongqing) Southwest Equipment Research Institute Co., Ltd, Chongqing, 401122, China

[2] China Shipbuilding (ChongQing) Equipment Technology Co., Ltd, Chongqing, 401122, China

[3] CISDI Information Technology (Chongqing) Co.,Ltd, Chongqing, 401122, China

[*]Corresponding Author

Abstract

This study investigates a compact Integrated High-Temperature Upper Bonnet by quantifying how cooling-fin geometry affects the valve-stem packing gland and setting optimization priorities for high-temperature valves. A 3D steady-state thermal model was built in ANSYS Workbench using the Finite Element Method and evaluated under 525 °C process gas. Orthogonal Experimental Design with range analysis assessed fin number, fin diameter depth, and fin spacing. Simulations show that heat conduction across the 1.5 mm stem-to-bonnet gap must be modeled; otherwise the packing-gland peak temperature is overestimated by up to 15.7%. Benchmarking indicates the integrated bonnet (235 mm) matches the cooling of a traditional extended bonnet (380 mm) while reducing height by 38.2%. Parameter influence ranks as fin number (R_A = 36.89) > fin diameter depth (R_B = 21.12) > fin spacing (R_C = 9.50), identifying fin number as the primary design lever. These results validate the integrated bonnet's thermal performance and compactness and provide quantitative evidence for design and safety certification of high-temperature industrial valve accessories.

Keywords

Integrated High-Temperature Upper Bonnet; Finite Element Method; Orthogonal Optimization; Cooling Fin; Heat Dissipation; Packing Gland Temperature.

1. Introduction

1.1 Origin and Development of High-Temperature Valve Heat Dissipation Research

In high-temperature and high-pressure industrial sectors such as petrochemical, power generation, and metallurgy, the valve serves as a critical fluid control device, whose reliability directly impacts the safety and efficiency of the entire system. High-temperature media impose stringent thermal management requirements on the main body of the valve and its components, such as the bonnet, packing gland, and actuator. Excessive temperatures not only lead to a decrease in material strength and hardness, accelerating high-temperature creep, corrosion, and thermal stress fatigue, but also severely compromise the sealing performance of the stem packing, potentially causing control signal distortion and system failure[1-3]. Consequently, high-temperature thermal management of valves has consistently been a focal point in the fields of fluid machinery and heat transfer.

Earlier thermal analysis studies primarily focused on critical moving parts like internal combustion engine exhaust valves, employing thermo-structural coupling analysis to predict temperature fields

ISSN: 2414-1895 DOI: 10.6919/ICJE.202511_11(11).0017

and thermal stress distribution[4-6]. Researchers have utilized the Finite Element Method (FEM) for thermal analysis of valves, for instance, conducting computational thermal stress analysis on high-pressure control valve bodies to evaluate their structural integrity under high-temperature conditions[7, 8]. As industrial demands for temperature and pressure continue to rise, traditional valve structures, such as the standard extended bonnet, often fall short of meeting the rigorous heat dissipation requirements. This has driven the application and optimization of more efficient extended surface heat dissipation technology, specifically cooling fins (radiating plates), on industrial valves[9, 10].

1.2 Current Status of Valve Heat Dissipation Structure and Optimization Methods

In recent years, research on high-temperature valve heat dissipation structures has mainly concentrated on two aspects: the adoption of new cooling technologies and materials, and the application of advanced numerical simulation and optimization methods. In terms of novel cooling, researchers have explored the use of new material coatings to enhance the thermal performance of valve components[4], and applied high-efficiency liquid cooling techniques (e.g., microchannel cold plates, Tesla valve channels) in fields like electric vehicles. Although the application objects differ, their design concept of high heat transfer efficiency offers valuable insights for improving industrial valve heat dissipation structures[11, 12]. These studies demonstrate that through optimizing the flow channel and structure, higher heat transfer efficiency and lower pressure drop can be achieved[13].

In addition to these advancements, Computational Fluid Dynamics (CFD) and Finite Element Analysis (FEA) have become standard tools for high-temperature valve thermal analysis, enabling accurate prediction of complex temperature fields and heat flux distribution[2, 14]. Crucially, to identify the optimal heat dissipation solution under the influence of multiple factors, Design of Experiment (DOE) methods, particularly Orthogonal Test and Multi-Objective Optimization algorithms, have been widely adopted[12, 15]. For example, researchers have optimized the geometric parameters of cooling fins through orthogonal experiments to balance heat dissipation performance and flow resistance[9]. These studies have significantly promoted the shift in heat dissipation structure design from empirical guidance to quantitative optimization, providing a theoretical foundation for achieving high-performance valve thermal management[16].

1.3 Shortcomings and Significance of This Study

Despite the extensive domestic and international research on high-temperature valves and heat dissipation structures, the following gaps persist: Firstly, a large volume of existing research focuses on engine valves or complex heat exchanger structures, with relatively limited studies on the thermal characteristics of the specific geometry of the integrated high-temperature top bonnet (a heat dissipation form used in industrial control valves designed to simplify the structure and reduce height). Secondly, there is a lack of systematic, DOE-based quantitative analysis regarding the primary and secondary influence of key heat dissipation structural parameters (such as the number, diameter, and spacing of cooling fins) in industrial applications. This lack of information leaves engineering designers without reliable guidance when balancing structural compactness against heat dissipation performance.

In light of these shortcomings, this study focuses on the integrated high-temperature top bonnet structure under high-temperature operating conditions, conducting temperature field simulation and orthogonal analysis. The aims of this research are: 1) to accurately simulate the temperature field distribution of this structure when exposed to high-temperature gaseous media; 2) to systematically quantify the degree of influence of key geometric parameters such as the number, diameter, and spacing of the cooling fins on the heat dissipation performance using the Orthogonal Test method; and 3) to clearly identify the maximum influencing factor affecting the heat dissipation of the integrated high-temperature top bonnet, with the goal of providing optimal design criteria for engineering applications. This research not only enriches the theoretical foundation in the field of thermal management for high-temperature industrial valve accessories but also offers significant

ISSN: 2414-1895 DOI: 10.6919/ICJE.202511_11(11).0017

guidance for enhancing the practical application value and engineering design efficiency of the new integrated top bonnet.

1.4 Outline of the Study

This paper first establishes a three-dimensional model of the integrated high-temperature top bonnet and performs temperature field simulations based on the ANSYS Workbench platform. Subsequently, the Orthogonal Test method is used to design the experimental plan, and range analysis is performed on the simulation results to determine the primary and secondary order of influence of different cooling fin structural parameters on the bonnet's heat dissipation effect. Finally, based on the analysis results, suggestions for optimizing the heat dissipation structure of the integrated high-temperature top bonnet are proposed, and corresponding conclusions are drawn.

2. Theoretical Foundation

This study aims to address the heat dissipation problem of the integrated high-temperature top bonnet by combining numerical simulation and optimization design methods. Its theoretical foundation primarily covers the complex heat transfer mechanisms in high-temperature components, the principle of numerical solution based on the Finite Element Method (FEM), and the theory of Orthogonal Experimental Design for multi-factor optimization.

2.1 Heat Transfer Model for High-Temperature Valve Components

The heat dissipation process of the integrated high-temperature top bonnet is a complex three-dimensional, transient thermodynamic process involving three fundamental modes of heat transfer: conduction, convection, and radiation. For the purpose of this study, a steady-state simulation is adopted, where the temperature field distribution within the bonnet must satisfy the law of energy conservation.

2.1.1. Governing Equation for Steady-State Heat Conduction

Heat transfer from the high-temperature medium side through the valve body and bonnet material to the external environment is predominantly by conduction. In isotropic materials with no internal heat generation, the steady-state heat conduction process must satisfy the following differential equation (the simplified form of the energy conservation equation):

$$\frac{\partial}{\partial x}\left(k\frac{\partial T}{\partial x}\right)+\frac{\partial}{\partial y}\left(k\frac{\partial T}{\partial y}\right)+\frac{\partial}{\partial z}\left(k\frac{\partial T}{\partial z}\right)=0$$

where T is the temperature, k is the thermal conductivity of the material, and x, y, z are the spatial coordinates. The objective of this study is to determine the temperature distribution $T(x, y, z)$ within the entire bonnet domain Ω.

2.1.2. Convection and Radiation Heat Transfer Boundary Conditions

The outer surface of the bonnet exchanges heat with the surrounding air via natural convection. This boundary condition is described by Newton’s law of cooling:

$$-k\frac{\partial T}{\partial \mathbf{n}}=h_{\text{conv}}(T_w-T_a)$$

Here, $\mathbf{n}$ is the normal direction to the outer surface, h_{conv} is the convection heat transfer coefficient, T_w is the wall temperature, and T_a is the ambient temperature. Due to the high operating temperature of the bonnet, the effect of **thermal radiation** cannot be ignored. The radiation heat transfer boundary condition is described by the Stefan-Boltzmann law:

ISSN: 2414-1895 DOI: 10.6919/ICJE.202511_11(11).0017

$$-k\frac{\partial T}{\partial \mathbf{n}} = h_{\text{rad}}(T_w - T_a) = \varepsilon\sigma(T_w^4 - T_a^4)$$

where h_{rad} is the radiation heat transfer coefficient, ε is the surface emissivity, and σ is the Stefan-Boltzmann constant. In numerical simulation, the combined effect of convection and radiation is often simplified using a total equivalent heat transfer coefficient $h_{\text{total}} = h_{\text{conv}} + h_{\text{rad}}$ for finite element analysis.

2.2 Numerical Analysis Based on the Finite Element Method

This study utilizes the ANSYS Workbench platform for temperature field analysis, the core of which relies on the Finite Element Method (FEM) to discretize and solve the aforementioned governing equation and boundary conditions.

The FEM discretizes the continuous solution domain (the valve bonnet geometric model)[Figure 1] into a finite number of elements (mesh)[Figure 2].

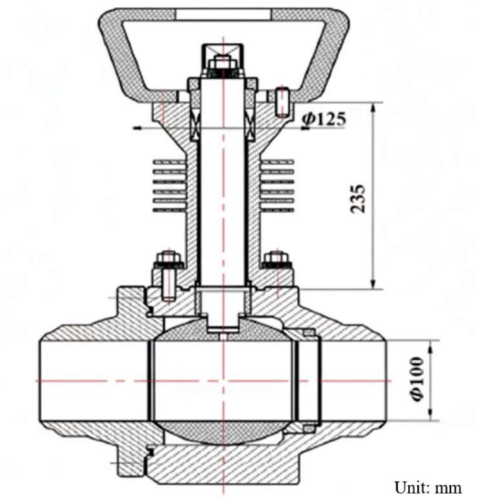

Figure 1. Assembly diagram of integral high temperature upper bonnet

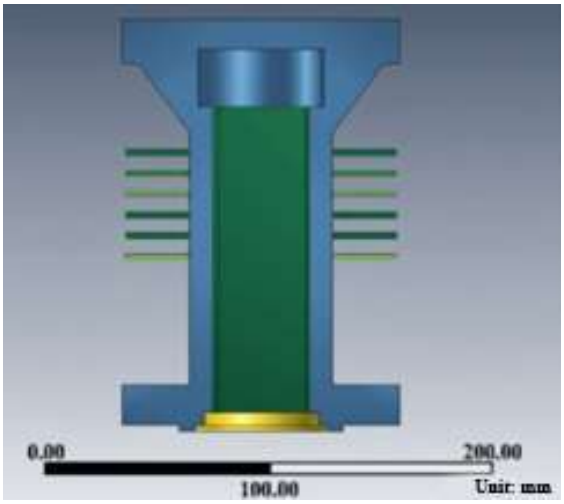

Figure 2. Schematic diagram of simulation model

Within each element, the temperature field $T(x, y, z)$ is approximated through interpolation functions based on nodal temperatures. Consequently, the continuous heat conduction problem is transformed into a large system of linear or non-linear algebraic equations for solution:

ISSN: 2414-1895 DOI: 10.6919/ICJE.202511_11(11).0017

$$[\mathbf{K}]\{\mathbf{T}\} = \{\mathbf{F}\}$$

In this system, $[\mathbf{K}]$ is the global heat conduction (stiffness) matrix, constructed from the element thermal conductivities and geometric properties; $\{\mathbf{T}\}$ is the vector of unknown nodal temperatures; and $\{\mathbf{F}\}$ is the global thermal load vector, which incorporates the effects of boundary conditions such as thermal convection and radiation. Solving this system yields the overall temperature distribution of the bonnet and allows for the extraction of temperatures at critical locations, such as the valve stem packing, as the optimization objective.

2.3 Orthogonal Experimental Design and Range Analysis Theory

To efficiently determine the primary and secondary influence of key structural parameters (fin number A, diameter B, spacing C) on heat dissipation performance and identify the optimal combination, the study employs Orthogonal Experimental Design and the Range Analysis Method.

2.3.1. Orthogonal Experimental Design

Orthogonal Experimental Design is an optimization method used to study experiments with multiple factors and multiple levels. It utilizes an Orthogonal Array $L_N(Q^K)$, which possesses a "balanced and scattered" property, to arrange the experiments. N is the number of trials, Q is the number of levels, and K is the number of factors. By selecting a minimal set of representative experiments[Table 1], the method can obtain the maximum amount of information with the fewest trials, ensuring uniformity and comparability among factor level combinations.

Table 1. Grid independence verification

Number of cells	Maximum temperature at packing bottom (℃)
4991	93.63
7644	95.12
12635	96.49
18320	96.69

2.3.2. Range Analysis Method

The Range Analysis Method is a common statistical technique for interpreting the results of orthogonal experiments. First, the average result $\overline{K}_{j,i}$ for the performance index under the i-th level of the j-th factor is calculated:

$$\overline{K}_{j,i} = \frac{1}{n_i}\sum_{l=1}^{n_i} Y_{j,l}$$

where $\overline{K}_{j,i}$ is the average performance index (e.g., temperature at the valve stem packing) for the j-th factor (e.g., fin number) at the i-th level, $Y_{j,l}$ is the performance index of the l-th experiment included in that level, and n_i is the number of trials at that level.

Next, the Range R_j for each factor is calculated:

$$R_j = \max(\overline{K}_{j,1}, \overline{K}_{j,2}, \dots) - \min(\overline{K}_{j,1}, \overline{K}_{j,2}, \dots)$$

ISSN: 2414-1895 DOI: 10.6919/ICJE.202511_11(11).0017

A larger value of the Range R_j indicates a more significant influence of that factor (j) on the performance index. By comparing the magnitudes of R_A, R_B, R_C, the primary and secondary influence relationship of fin number, diameter, and spacing on the integrated high-temperature top bonnet's heat dissipation performance is determined.

3. Simulation Analysis of Heat Dissipation on Integral High Temperature Upper Bonnet

3.1 Simulation Boundary Conditions and Parameter Settings

The temperature field simulation in this study was based on the following key boundary conditions and parameter settings, designed to accurately model the heat dissipation process of the integrated high-temperature upper bonnet under actual industrial conditions.

3.1.1. Medium and Ambient Conditions

Internal Medium: High-temperature process gas (DN100 Class150 specification).

Medium Temperature T_{in}: $525°C$.

Ambient Temperature T_{a}: $25°C$.

Material Properties: The bonnet body, valve stem, packing gland, and other components were all modeled using 1Cr18Ni9Ti stainless steel, with a thermal conductivity k set at $15.1\text{W}/(\text{m}\cdot\text{K})$, density ρ at $7850\text{kg}/\text{m}^3$, and specific heat capacity c at $460\text{J}/(\text{kg}\cdot\text{K})$.

3.1.2. Heat Transfer Boundary Conditions

The simulation fully accounted for both natural convection and thermal radiation for external heat transfer:

Convection Heat Transfer Coefficient h_{conv}: Set at $5\text{W}/(\text{m}^2\cdot\text{K})$.

Surface Emissivity ε: The emissivity ε for thermal radiation between the bonnet outer surface and the air was set to 0.8.

Total Heat Transfer Rate Q_{total}: The combined heat transfer rate, considering both convection and radiation, is expressed as:

$$Q_{\text{total}} = A \cdot (h_{\text{conv}}(T_w - T_a) + \varepsilon\sigma(T_w^4 - T_a^4))$$

where A is the heat transfer area, T_w is the wall temperature, T_a is the ambient temperature, and σ is the Stefan-Boltzmann constant.

Internal Thermal Boundary: The internal surface of the bonnet (contacting the high-temperature medium) was set to $525°C$. A critical consideration was the small gap between the valve stem and the bonnet (1.5 mm on one side), where the heat conduction effect of the medium within the gap was explicitly included in the model.

3.2 Influence of Medium on Heat Dissipation in the Gap between Valve Stem and Upper Bonnet

This study performed a simulation analysis for a valve operating with high-temperature gas medium ($525°C$ process gas). Since high-temperature gases have extremely low thermal conductivity and the gap between the valve stem and the upper bonnet (1.5 mm on one side) is small, the heat transfer within this gap primarily occurs via heat conduction (assuming no phase change). This analysis aimed to verify the impact of gap medium heat transfer on the packing gland temperature.

Temperature Result without Gap Medium: The maximum temperature at the packing gland bottom, when neglecting heat transfer by the medium in the gap, was 111.76℃[Figure 3(a)].

ISSN: 2414-1895 DOI: 10.6919/ICJE.202511_11(11).0017

Temperature Result with Gap Medium: When fully considering the heat conduction effect of the medium within the gap, the maximum temperature at the packing gland bottom decreased to 96.608℃[Figure 3(b)].

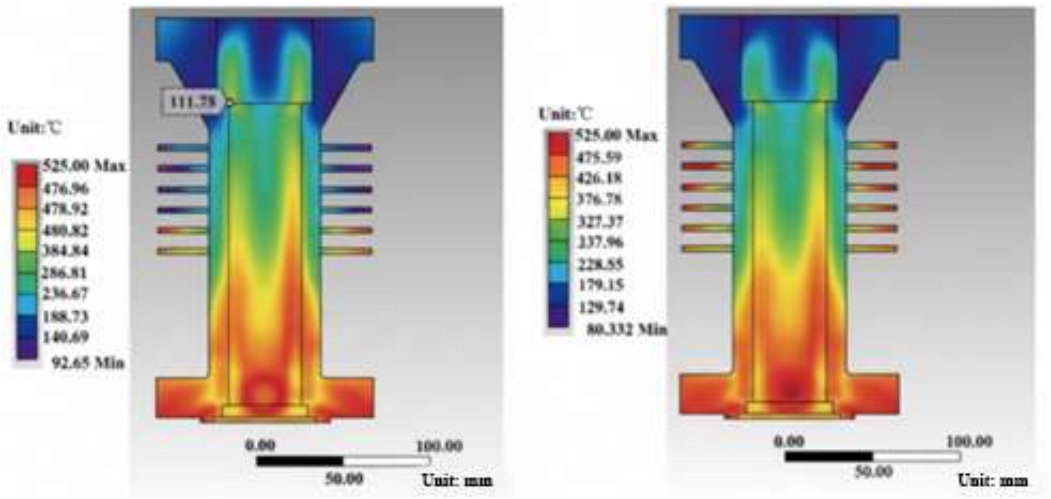

(a) (b)

Figure 3. Temperature distribution with or without medium in clearance

Discrepancy: The maximum temperatures differed by 15.7% (111.76℃ vs 96.608℃) between the two scenarios.

Intensity of Heat Transfer in the Gap: As illustrated in Figure 5, within the thin 1.5 mm medium layer, the temperature drastically drops from 232.75℃ (contacting the stem) to 96.61℃ (contacting the upper bonnet)[Figure 4].

Conclusion: The simulation results confirm that for high-temperature gas medium conditions, the heat conduction effect of the medium in the gap between the valve stem and the upper bonnet is a critical factor influencing the packing gland temperature and must not be ignored.

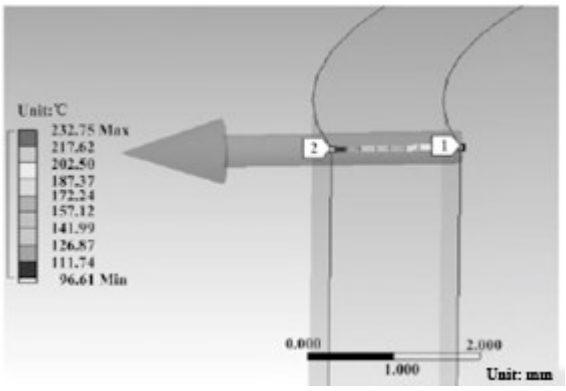

Figure 4. Radial heat conduction diagram of medium layer

3.3 Comparative Heat Dissipation Effectiveness of the Integral High Temperature Upper Bonnet

This section compares the integrated high-temperature top bonnet structure with the traditional extended upper bonnet structure based on structural height required to achieve similar heat dissipation performance.

Integrated High Temperature Upper Bonnet (Structure under Study): The bonnet height is 235 mm[Figure 1], and the maximum temperature at the packing gland bottom is 96.608℃[Figure 3(b)].

ISSN: 2414-1895 DOI: 10.6919/ICJE.202511_11(11).0017

Traditional Extended Upper Bonnet: To achieve a similar cooling effect (maximum temperature of 94.729℃), the required height for the extended bonnet is 380 mm[Figure 5].

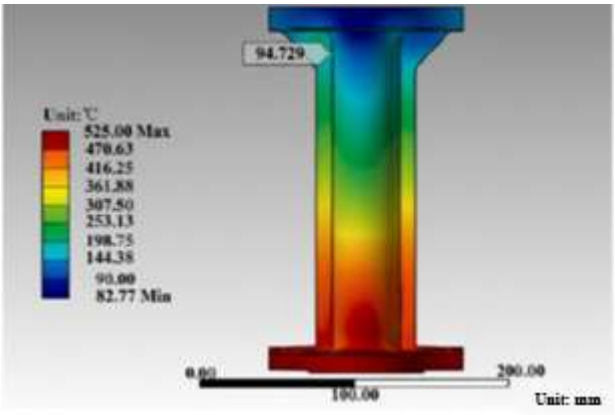

Figure 5. Temperature distribution of extended upper bonnet

Conclusion: The integrated high-temperature upper bonnet structure achieves a comparable temperature at the packing gland bottom (96.608℃ vs 94.729℃) while reducing the structure height by 38.2% (calculated as $1 - 235/380 \approx 0.382$) compared to the traditional extended bonnet (380 mm). This indicates a significant benefit in terms of structural simplification and cost efficiency.

3.4 Analysis of Influence Factors on Integral High Temperature Upper Bonnet Heat Dissipation

To quantify the influence of various design parameters on heat dissipation performance, this study utilized the Orthogonal Analysis Method for experimental design and data analysis. The performance index was the maximum temperature at the packing gland bottom, with the objective of minimizing this temperature.

3.4.1. Orthogonal Test Factors and Level Settings

A 3-factor, 3-level orthogonal array was used for the analysis[Table 2]. The factors and their assigned levels were:

Factor A: Number of cooling fins, with levels $A_1 = 7,\ A_2 = 5,\ A_3 = 3$.

Factor B: Diameter depth of cooling fins (mm), with levels $B_1 = 29,\ B_2 = 25,\ B_3 = 21$.

Factor C: Spacing between cooling fins (mm), with levels $C_1 = 29,\ C_2 = 25,\ C_3 = 21$.

Table 2. Orthogonal analysis table of four factors and three levels

No.	Heat sink plate quantity (A)	Heat sink plate diameter (B) / mm	Heat sink plate pitch (C) / mm	Maximum temperature at packing bottom (℃)
1	A1	B1	C1	93.77
2	A1	B2	C2	98.15
3	A1	B3	C3	105.28
4	A2	B1	C2	105.54
5	A2	B2	C3	111.68
6	A2	B3	C1	118.61
7	A3	B1	C3	136.92
8	A3	B2	C1	143.58
9	A3	B3	C2	142.53

ISSN: 2414-1895 DOI: 10.6919/ICJE.202511_11(11).0017

3.4.2. Range Analysis Results

Based on the orthogonal test results[Table 2], the average temperature ($\overline{K}$) for each factor at different levels was calculated, and the Range (R) was determined.

1) Range Calculation for Factor A (Fin Number):

The average temperatures for the levels of factor A were:

$$\overline{K}_{A_1} = \frac{93.77 + 98.15 + 105.28}{3} \approx 99.07(^{\circ}C)$$
$$\overline{K}_{A_2} = \frac{105.54 + 111.68 + 143.38}{3} = 120.2(^{\circ}C)$$
$$\overline{K}_{A_3} = \frac{128.52 + 136.82 + 142.53}{3} \approx 135.96(^{\circ}C)$$

The Range for factor A was:

$$R_A = \max(\overline{K}_{A_1}, \overline{K}_{A_2}, \overline{K}_{A_3}) - \min(\overline{K}_{A_1}, \overline{K}_{A_2}, \overline{K}_{A_3}) = 135.96 - 99.07 = 36.89$$

2) Range Calculations for Factor B (Fin Diameter Depth) and Factor C (Fin Spacing):

The Range for factor B was calculated as:

$$R_B = 21.12$$

The Range for factor C was calculated as:

$$R_C = 9.50$$

3.4.3. Conclusion and Interpretation

Order of Influence: Comparing the Range values of the factors yields the relationship $R_A > R_B > R_C$ $(36.89 > 21.12 > 9.50)$. This demonstrates that the degree of influence on the heat dissipation effectiveness of the integrated high-temperature top bonnet is ordered as follows: Fin Number (A) > Fin Diameter Depth (B) > Fin Spacing (C). The fin number is identified as the biggest influence factor.

Optimal Design Trend: The average temperature results ($\overline{K}$) indicate that the maximum temperature at the packing gland bottom decreases as the fin number increases, the fin diameter increases, and the fin spacing increases. Therefore, the optimal design tendency is that more fins, larger fin diameter, and larger fin spacing are conducive to heat dissipation. In practical design, priority should be given to increasing the number of fins to meet heat dissipation requirements.

4. Conclusion

This paper conducted a systematic thermal simulation and optimization study on a novel Integrated High-Temperature Upper Bonnet structure using the Finite Element Method on the ANSYS Workbench platform. The study aimed to quantify the cooling effect of key fin geometric parameters on the packing gland temperature and provide a theoretical basis for structural optimization.

4.1 Summary of Key Research Methods, Data, and Achievements

Numerical Simulation and Model Validation: This study successfully established a thermal model for the integrated high-temperature upper bonnet. Comparative analysis (with/without heat transfer by the gap medium) first demonstrated that under high-temperature gas medium $(525^{\circ}C)$ conditions,

ISSN: 2414-1895 DOI: 10.6919/ICJE.202511_11(11).0017

heat conduction by the medium in the 1.5mm gap between the stem and the bonnet is a critical heat dissipation path, and ignoring this effect leads to a significant 15.7% overestimation of the packing gland's maximum temperature ($111.76°C$ vs $96.608°C$).

Structural Efficiency Comparison: Simulation results confirmed that the integrated high-temperature upper bonnet structure (height 235mm) achieved a required temperature target (packing gland maximum temperature below $100°C$, $96.608°C$ vs $94.729°C$ for the traditional design) while reducing the structural **height** by 38.2% compared to the traditional extended upper bonnet structure (height 380mm).

Key Factor Quantification: Utilizing $L_9(3^3)$ Orthogonal Experimental Design and Range Analysis, the influence of fin geometric parameters was systematically quantified. The range analysis results showed that the influence of Fin Number ($R_A = 36.89$), Fin Diameter Depth ($R_B = 21.12$), and Fin Spacing ($R_C = 9.50$) on heat dissipation effectiveness followed the primary, secondary, and tertiary order, respectively.

4.2 Practical and Physical Conclusions

Structural Design Priority: The fin number is the most decisive factor (R_A is the largest) affecting the heat dissipation performance of the integrated high-temperature upper bonnet. In engineering practice, subject to spatial and manufacturing cost constraints, increasing the number of fins should be the primary heat dissipation design strategy.

Packing Gland Temperature Control: The temperature at the base of the packing gland is a crucial indicator of valve reliability. The optimal design trend identified by the simulation results favors a configuration with the maximum number of fins, maximum fin diameter depth, and maximum fin spacing.

Model Accuracy Requirement: For thermal analysis involving high-temperature, small-gap, and low-thermal-conductivity media in valve components, the heat conduction of the medium layer within the fluid-solid coupling interface must be included as a boundary condition in the finite element model. Failure to do so leads to a serious underestimation of the actual safe temperature margin for the packing gland.

References

[1] SERALATHAN, S., SANTHOSH, G. B., SIVANANDAM, P. Thermal analysis on different exhaust valve materials of compression ignition engine[J]. Materials Today: Proceedings, 2020, 33(3): 4105-4111. DOI: 10.1016/j.matpr.2020.06.550.

[2] LIU, L., ZHANG, L., YANG, D., et al. Two-phase flow-based numerical investigation of the temperature maps of sodium-cooled exhaust valves in a turbocharged engine[J]. Applied Thermal Engineering, 2020, 181: 115977. DOI: 10.1016/j.applthermaleng.2020.115977.

[3] YONG, M., KU, P. X. Study on the performance characteristics and failure analysis of exhaust valves[C]//Journal of Physics: Conference Series. Bristol: IOP Publishing, 2023, 2523(1): 012047.

[4] SIVAKUMAR, E. R., KRISHNA, R., SENTHILKUMAR, P., et al. Comprehensive study of diesel engine characteristics of valves coated by titanium nitride (TiN)[J]. Proceedings of the Institution of Mechanical Engineers, Part E: Journal of Process Mechanical Engineering, 2023: 09544089231157950. DOI: 10.1177/09544089231157950.

[5] XU, L., LIN, H., HU, N., et al. Multi-Objective Optimization towards Heat Dissipation Performance of the New Tesla Valve Channels with Partitions in a Liquid-Cooled Plate[J]. Energies, 2024, 17(13): 3106. DOI: 10.3390/en17133106.

[6] CHENG, J., WANG, Z., GUO, J., et al. Thermal-mechanical coupling analysis of high-temperature control valve bonnet under transient conditions[J]. Journal of Mechanical Engineering, 2021, 57(12): 101-110.

[7] UDIN, S. M. K., HASAN, N. Enhanced Thermal Performance Analysis Of Engine Cooling Fins With Varying Geometries And Materials[J]. International Journal of Mechanical and Production Engineering Research and Development, 2024, 14(1): 164-173.

ISSN: 2414-1895 DOI: 10.6919/ICJE.202511_11(11).0017

[8] ZHAO, K., CHEN, W., WANG, H., et al. Optimization of Heat Transfer and Flow Performance of Microchannel Liquid-Cooled Plate Based on Orthogonal Test[J]. Sustainability, 2023, 15(6): 905. DOI: 10.3390/su15060905.

[9] SILVA, C. T. B., OLIVEIRA, A. P. Analysis of the temperature and stress distributions on an automotive valve train due to friction effects[J]. International Journal of Engineering Research and Applications, 2020, 10(7): 20-27.

[10] MAVROPOULOS, G., MARKOPOULOS, A. G., TSANAS, A. Heat Losses in the Exhaust Manifold of a 4-Stoke DI Diesel Engine Subjected to Pulsating Flow[J]. Journal of Sustainable Energy, 2024, 13(9): 223. DOI: 10.3390/su1309223.

[11] AHMED, S. S. H. S., ALI, W. J. Investigation of the Effect of Different Fins Configurations on the Thermal Performance of the Radiator[C]//Journal of Physics: Conference Series. Bristol: IOP Publishing, 2024, 2733(1): 012028.

[12] CHEN, X., FAN, H., MA, J., et al. Innovative Designs of 3D Heat Sinks by Topology Optimization[J]. Journal of Mechanical Design, 2024, 147(8): 081705. DOI: 10.1115/1.4065600.

[13] ZHU, Z., SHEN, H., WANG, Z., et al. Thermal stress analysis of high-temperature high-pressure butterfly valve body[J]. Fluid Machinery, 2022, 50(11): 45-50.

[14] ALWAN, H. G., MOHAMMAD, H. K. Enhancement of Heat Transfer from Extended Surfaces (Fins): A Comprehensive Review[J]. International Journal of Thermal Sciences, 2023, 187: 108154. DOI: 10.1016/j.ijthermalsci.2023.108154.

[15] QASIM, T. M., ABBAS, H. T. Computational thermal stress analysis of control valve body using finite element method[J]. Journal of Engineering Science and Technology, 2022, 17(2): 1104-1117.

[16] GOUDARZI, S. A. Effect of contact pressure and frequency on contact heat transfer between exhaust valve and its seat[J]. International Journal of Engineering-Transactions B: Applications, 2020, 33(3): 401-408. DOI: 10.5829/ije.2020.33.03c.12.